β decay of ^{49,50}Ar

L. Weissman,[1] U. Bergmann,[2] J. Cederkall,[2] L. M. Fraile,[2,*] S. Franchoo,[2] H. Fynbo,[1,3] H. Gausemel,[4] H. Jeppesen,[3] U. Köster,[2] K.-L. Kratz,[5] T. Nilsson,[2] B. Pfeiffer,[5] K. Van del Vel,[6] and ISOLDE Collaboration

[1]*NSCL, Michigan State University, East Lansing, Michigan 48824, USA*

[2]*ISOLDE, CERN, CH-1211 Geneva 23, Switzerland*

[3]*Institut for Fysik og Astronomi, Aarhus Universitet, DK-8000 Aarhus C, Denmark*

[4]*Kjemisk Institutt, Universitetet i Oslo, Postboks 1033, Blinern, N-0315 Oslo, Norway*

[5]*Instituut voor Kern-en Strlingsfysica, K.U. Leuven, 3001 Leuven, Belgium*

[6]*Institut für Kernchemie, Universität Mainz, 55128 Mainz, Germany*

(Received 18 February 2003; published 27 May 2003)

Information on gross β-decay properties of neutron-rich noble gas isotopes ^{49,50}Ar was obtained at the PSB-ISOLDE facility at CERN using isobaric selectivity achieved by the combination of a plasma ion source with a cooled transfer line and subsequent mass separation. A doubly charged beam was used in the case of ^{49}Ar to suppress the corresponding multicharged background from heavier noble gas fission products. The comparison of the obtained data with results of quasiparticle random-phase approximation calculations indicates that the $N=28$ shell is not disturbed significantly for neutron-rich Ar nuclei. The obtained results are useful for better understanding of the origin of the ^{48}Ca/^{46}Ca isotopic anomaly discovered in inclusions from the Allende meteorite.

DOI: 10.1103/PhysRevC.67.054314 PACS number(s): 23.40.−s, 27.40.+z

I. INTRODUCTION

The interest in the nuclear structure of the neutron-rich nuclei around doubly magic ^{48}Ca has both nuclear physics and astrophysics origins. The experimental data from GANIL and NSCL indicate a significant degree of collectivity in the corresponding $N=28$ sulfur and chlorine isotopes [1–4]. On the other hand the effect of the $N=28$ shell closure persists in ^{46}Ar [3]. The mass region of interest is quite challenging for theoretical calculations due to the ''soft'' potential-energy surface that results in rapid nuclear-shape changes. In general, several recent theoretical studies [5–10] have confirmed the experimental results. Nevertheless, a few questions regarding the origin of the observed collectivity are still open. For example, it is not completely clear whether the observed collectivity has static or vibrational origin [11]. It is also argued that the investigated isotopes are collective due to shifts in the proton single particle energies rather than weakening of the $N=28$ shell [12]. Therefore new experimental information is highly desirable for further investigation of the region. In this context, the heavier neutron-rich argon isotopes are of considerable interest.

Knowledge of the nuclear properties of these isotopes is also important for understanding a long persisting astrophysical puzzle, the Ca/Ti/Cr isotopic anomalies observed in some meteoritic inclusions. Especially striking isotopic anomalies were discovered in the refractory inclusions of the Allende meteorite [13,14] where the ratio of abundances of the ^{48}Ca/^{46}Ca isotopes was found to be approximately five times higher than the corresponding value for the solar system. These meteorite inclusions, most likely, were formed from not completely mixed matter at the earliest stage of the solar nebula; therefore, they may provide unique information on specific nucleosynthesis processes. For the most plausible astrophysical scenario, the $Z\leqslant 20$ and $N\approx 28$ neutron-rich isotopes are the progenitors of the stable ^{48,46}Ca, therefore, their nuclear properties are important input parameters for astrophysical network calculations [15]. In most of the cases even the gross nuclear decay properties, such as half-lives and neutron emission probabilities, P_n, are very useful. This was demonstrated in experimental studies performed at GANIL and ISOLDE where half-lives and P_n values of the neutron-rich $^{48-51}$K, ^{43}P, $^{42-45}$S, $^{44-46}$Cl, and ^{47}Ar isotopes were measured [1,2,16–18]. At present, the decay properties of neutron-rich argon isotopes are the least known compared to other nuclei relevant to the ^{48}Ca/^{46}Ca anomaly. As ^{48}Ar is the main progenitor of the ^{48}Ca isotope, the lack of information on its decay properties limits considerably the predictive power of the astrophysical network calculations [15].

Even though the neutron-rich argon isotopes were observed at GANIL up to ^{51}Ar by fragmentation of a 55 MeV/nucleon ^{48}Ca beam [19], the low yields obtained for very neutron-rich fragmentation products made it difficult to perform reliable measurements at that time. The neutron-rich Ar nuclei can also be produced at ISOL facilities. For instance, bombardment of a standard ISOLDE uranium carbide target with a 1–1.4 GeV proton beam from the CERN proton synchrotron booster (PSB) facility provides sufficient yields of neutron-rich asymmetric fission (ASF) argon products [20] to perform such a measurement. However, a number of experimental difficulties significantly hinder such measurements. While mixed beams of radioactive nuclei can be used at fragmentation facilities, where measurements of energy losses and time of flight allow unambiguous identification of various species, such a measurement at an ISOL facility re-

*On leave from Dept. de Física Atómica, Molecular y Nuclear, Universidad Complutense, E-28040 Madrid, Spain.

quires high purity of the radioactive beam. This purity can be achieved only by using the chemically selective ion sources. In general, ionization of noble gas products is difficult and requires chemically nonselective plasma ion sources that ionize the whole isobaric chain. Using a cooled transfer line between the target and the ion source adds the necessary element selectivity by condensing and depositing all nonvolatile reaction products, except the noble gases. Thus, only noble and some other gas products are transported via the cooled line, ionized in a plasma ion source, and subsequently extracted and mass separated. The extracted singly charged ASF argon products, however, cannot be mass separated from multiply charged krypton and xenon symmetric fission (SF) noble gas products that have the same M/Q ratio. Even though the ionization efficiency of a plasma ion source is much lower for ionization of multiple charge states, the in-target SF productions are, in many cases, few orders of magnitude higher than the corresponding values for the ASF products. This results in an overwhelming doubly charged krypton and triply charged xenon background for the singly charged argon beam. This experimental problem may be responsible for the fact that since the earlier ^{45,46}Ar study [21] no significant progress has been made in the investigation of neutron-rich Ar isotopes using the ISOL method.[1]

An additional complication for the measurement of noble gases is their fast diffusion from the implantation materials. For a given implantation energy the fraction of diffused ions depends on the implantation host and the diffusion time varies considerably for different noble gas species [23]. Therefore, it is virtually impossible to extract information on the decay of an argon isotope only from β and neutron decay profiles when a cocktail of noble gas ions is implanted. A pure argon beam has to be produced for a reliable measurement.

In this paper we address a possible way to partly overcome the above mentioned experimental difficulties, and furthermore report on the experimental results for ^{49,50}Ar and discuss their implications.

II. EXPERIMENT AND RESULTS

Neutron-rich argon isotopes were produced in fission reactions induced by a pulsed beam of 1.4 GeV protons (3×10^{13} protons per pulse) from the PSB accelerator impinging on a standard ISOLDE uranium carbide target (50 g/cm^2 U).

The reaction products effused from the target heated to about 2000 °C via a low-temperature, water-cooled transfer line to a standard FEBIAD type plasma ion source, where the ionization by plasma discharge took place [24]. The temperature of the transfer line was kept at about 50 °C, providing efficient condensation of possible isobaric contaminants. A 95%/5% mixture of argon and xenon was used as support gas for the plasma discharge. The ratios of efficiencies of ionization for different charge states were determined for the three noble-gas elements by measuring mass separated currents. For the Ar^{+1}-Ar^{3+} and Xe^{+1}-Xe^{4+} mass-separated beams the relative efficiencies were measured with a standard Faraday cup. For the higher charged Xe and for the Kr beams the intensities of the mass-separated long-lived radioactive isotopes produced by proton bombardment of the target were measured with a β counter. The ratios were found to be: Ar^{+1}: Ar^{2+}: $Ar^{3+}=1050:125:1$, Kr^{+1}: Kr^{2+}: Kr^{3+}: $Kr^{4+}=60\,000:6000:30:1$, Xe^{+1}: Xe^{2+}: Xe^{3+}: Xe^{4+}: Xe^{5+}: $Xe^{6+}=300\,000:33\,000:5500:80:1:2.5$. The measured efficiency ratios strongly depend on various ion source parameters such as anode voltage, internal magnetic field, and target line temperature [25]. All source parameters were therefore kept unchanged during the measurements and the efficiency ratios obtained for the stable isotopes were assumed to be the same for the radioactive isotopes. The leakage of non-noble-gas elements through the cooled line was found to be negligible for the masses of interest.

The highest available, 1.4 GeV, energy of protons was chosen to enhance the ASF production in respect to the symmetric fission [26]. Ionized neutron-rich noble-gas isotopes were extracted, mass separated, and implanted into an aluminized mylar tape, which allowed to remove the long-lived daughter activity from the detector setup. The implantation point was situated in the center of a cylindrical 4π neutron long counter. The detector consists of 12 parallel-coupled ^{3}He proportional counters embedded in a paraffin moderator [27]. The implantation point was placed close to a 125-μm Kapton window transparent to high-energy β particles. A 1.5-mm-thick plastic detector was positioned close to the Kapton window for detection of β particles. Several 50-cm-long optical fibers guided the scintillation light to two photomultipliers placed outside the neutron counter barrel. Only coincidences between fast time signals from two photomultipliers were considered as a true detection of a β particle. This allowed for the reduction of random electronic noise to a level of the order of 1 Hz. The detection times of the thermalized neutrons and β particles were recorded by a precise time-stamping module based on a 10-MHz clock with 32 bits time resolution. Each registered event consisted of the time relative to the proton beam hitting the target, and a pattern word to indicate whether the event was triggered by a neutron or a β particle. This allowed to produce both ''singles'' time decay spectra of neutrons and betas independently, as well as β-neutron time correlations. The detection efficiency of the neutron long counter was measured with a calibrated Am(Li) neutron source and was found to be 19(1)%. The detected random neutron background was only 0.3 Hz. The efficiency of the β detector was calibrated by simultaneously fitting the β and neutron time spectra of the known ^{94,96}Kr isotopes [23] and by comparison of the number of neutron-β correlations with the number of neutron counts [28]. The β detector efficiency was found to be 5.5(10)%.

The yields of the singly charged argon isotopes are compared in Fig. 1(a) to the yields of the corresponding multicharged Kr and Xe symmetric fission contaminants. The latter were obtained by scaling the yields for singly charged Kr and Xe ions [23] with the measured ratios of ionization effi-

[1]An exception is a Brief Report on the half-life of ^{47}Ar [22].

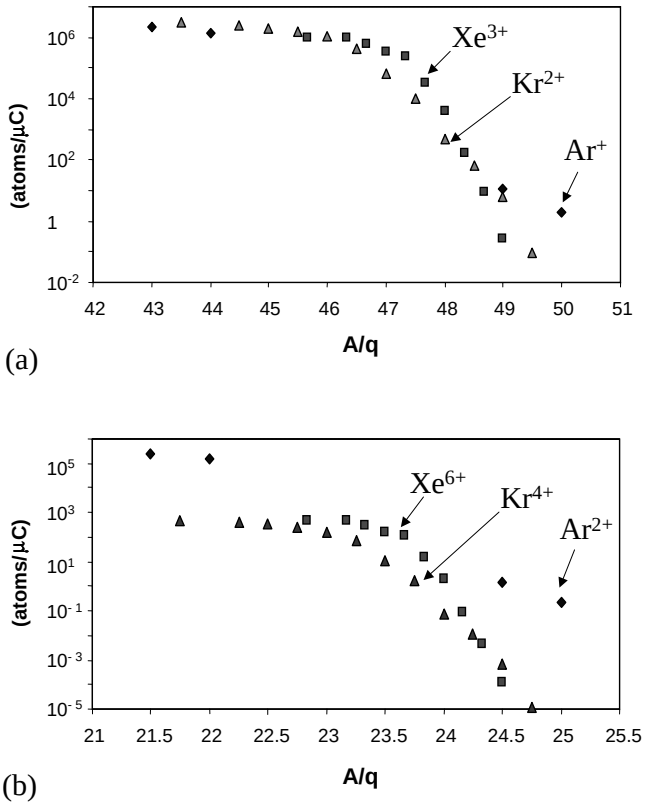

FIG. 1. (a) Comparison of the yields of singly charged argon (diamonds), doubly charged krypton (triangles), and triply charged xenon (squares) isotopes. b. The comparison of the yields of doubly charged argon (rhombus), quadruply charged krypton (triangles), and sextuply charged xenon (squares) isotopes.

ciencies for the corresponding charge states. The ^{43,44,49}Ar yields were measured for doubly charged ions (see below) with low multicharged SF background and subsequent scaling by the ratio of the singly and doubly charged ionization efficiencies. Due to the SF background it was not possible to determine the yield for ^{47,48}Ar, even with a doubly charged beam. The yield for ^{50}Ar was measured for a singly charged beam.

When the multicharged SF background is of the same magnitude as the yields of the ASF isotopes, the determination of decay properties, from the decay profiles, becomes virtually impossible due to the complexity of the fitting procedure. Only for the most exotic isotope, ^{50}Ar, the contaminations do not present a problem [Fig. 1(a)].

The situation can be improved for ^{49}Ar by mass separation of doubly charged argon ions. In this case the corresponding SF contaminations are quadruply charged krypton and sextuply charged xenon isotopes. Since the ionization efficiency is reduced significantly for the higher charge states the SF background is much lower. As is seen in Fig. 1(b), the doubly charged ^{49}Ar beam is practically clean from the SF contaminants. Thus a measurement for doubly charged ^{49}Ar can be performed though compromising significantly on the overall yield. The measurement of doubly charged ^{48}Ar is still hindered by multicharged fission products. In addition, it cannot be completely mass separated from a strong singly charged beam of the ^{24}Ne ASF product.

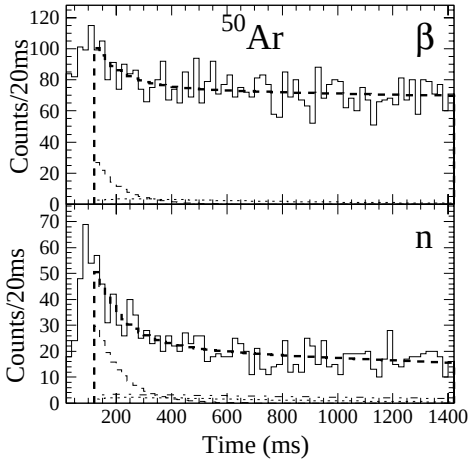

FIG. 2. The β and neutron decay time spectra measured for the singly charged ^{50}Ar beam. The constant background contribution to the fitting is not shown.

The time decay spectra measured in the β and neutron detectors for singly charged ^{50}Ar are presented in Fig. 2 together with the results of the fit. The beam-gate, i.e., the time period when ions were implanted, was set to 100 ms, and was opened after a short 10-ms delay following every proton pulse. The duration between proton pulses was 8.4 s. The tape was moved in 7 s after each proton pulse. A small fraction of ions, less than 5%, was implanted next to the tape, resulting in the buildup of a constant background of longer-lived activities in the β time spectrum. The measurement was performed during 5 h corresponding to 2150 proton pulses on the target. To verify the purity of the singly charged ^{50}Ar beam we have performed a short measurement at mass A=100. No signal from a singly charged ^{100}Kr was observed, ensuring the absence of doubly charged ^{100}Kr in the spectrum at mass $A=50$. The β and neutron spectra were fitted simultaneously by a decay chain that included ^{50}Ar, ^{50}K, ^{50}Ca, ^{50}Sc, ^{49}K, ^{49}Ca, and ^{49}Sc nuclei. A constant background was also included in the fit. The fitting procedure is described in detail in Ref. [23].

The half-lives and P_n values of the ^{50}Ar descendants were varied in the fit within the uncertainties tabulated in Ref. [29]. The efficiencies of the β and neutron detectors were varied in the fit within the limits deduced from the calibrations. The obtained values for the ^{50}Ar half-life and P_n value are 85(30) ms and 35(10)%, correspondingly.

As the analysis of the time spectra of the singly charged ^{49}Ar was hindered by the presence of a strong doubly charged ^{98}Kr component, only data for the doubly charged ^{49}Ar beam were taken. The beam-gate was set to be 200 ms after every proton pulse and a 20 ms delay. The β and neutron time decay spectra taken for the doubly charged ^{49}Ar beam are presented in Fig. 3 together with the results of the fit with the corresponding decay chains. The measurement was performed for 3 h (1320 proton pulses on the target). The values obtained from the fit for the half-life and neutron emission probability are 170(50) ms and 65(20)%, correspondingly.

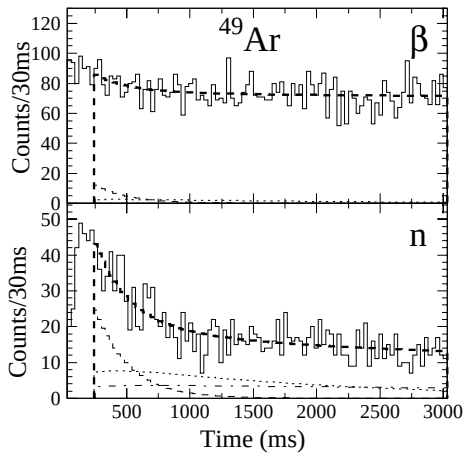

FIG. 3. The β and neutron decay time spectra measured for the doubly charged ^{49}Ar beam. The constant background contribution to the fitting is not shown.

The quality of the data for both the ^{49,50}Ar isotopes does not allow to perform a more careful analysis including the fraction of argon atoms that diffused from the tape. However, as was noticed in Ref. [23], the diffusion effect on the obtained half-lives is negligible if the duration of the collection time is larger than the time of diffusion. Comparing the diffusion times for He and Kr ions obtained in Ref. [23], the diffusion time of argon implanted at 60-keV energy can be estimated to be of the order of 50 ms. Therefore the above condition is satisfied for our data and the diffusion effect can be neglected within the experimental errors.

III. DISCUSSION

The major interest in the nuclear structure around ^{48}Ca is associated with the discovery of the rapid weakening of the $N=28$ shell in the ^{44}S and ^{45}Cl nuclei [1,2]. A few theoretical and experimental studies motivated by this experimental finding [3–6,8–10] pointed out towards large deformation in ^{44}S and neighboring lighter nuclei. However, the effect of the $N=28$ shell closure persists in the ^{46}Ar. There is quite a big uncertainty in the theoretical predictions for the heavier argon isotopes. The available theoretical predictions for ^{46,48,50}Ar include the large scale shell model calculations [8,10], the Hartree-Fock-Bogolyubov, and the relativistic mean-field (RMF) calculations [5,6], as well as predictions of the finite range droplet [30] and the extended Thomas-Fermi with the Strutinsky-integral models [31]. The predicted nuclear shapes for ^{48,50}Ar nuclei range from spherical to moderately oblate shapes with $\beta_2 \approx -0.25$. According to the theoretical description the nuclei of interest are γ soft in character [6,8], thus the extraction of nuclear deformation from the $B(E2)$ matrix elements measured in the Coulomb excitation experiments [3,4] is not a straightforward procedure.

Although one does not expect to obtain detailed information about nuclear structure from gross nuclear properties such as the β-decay half-life and β-delayed neutron probability, taken together these two values often lead to some first insights into nuclear structure. Both $T_{1/2}$ and P_n are determined by the β-strength function $S_\beta(E)$. While the half-life is dominated by the lowest-energy part in the β-strength function, the β-delayed neutron-emission probability is sensitive to feeding to the energy region just above the neutron separation energy S_n. Since $S_\beta(E)$ strongly depends on nuclear deformation, the measured $T_{1/2}$ and P_n do as well, but this dependence is not always trivial (see the discussion in Refs. [23,32]). Therefore information on nuclear structure may be obtained from the relative magnitude of $T_{1/2}$ and P_n. It can be accomplished by comparison of the experimental data with the results of theoretical calculations. The β-decay half-lives and β-delayed neutron-emission probabilities for ^{49,50}Ar were calculated using a microscopic quasiparticle random-phase approximation (QRPA), see Refs. [33–35], that has been enhanced to account for first-forbidden decays. The latter were calculated in the statistical gross theory [36,37]. Typical contribution of the first-forbidden decays in the β-strength function is of order of 10–15 %. The folded Yakawa potential and Lipkin-Nogami pairing interaction were used in the model [37]. As a first step, the β-strength distribution was calculated assuming a certain nuclear deformation. The half-lives were obtained by summing up all the transition probabilities to the states in the daughter nuclei within the Q_β energy window. The corresponding P_n values were calculated as the ratios of the sum of the transition probabilities to the high-lying states, above the neutron separation energy, to the sum of all transitions probabilities within the Q_β energy window. The procedure was repeated assuming different nuclear shapes from strongly oblate to strongly prolate values and, thus, the dependence of the calculated parameters on the nuclear deformation was obtained. The Q_β and S_n values used for these calculations were taken from the calculated masses [30,34]. The nuclear shapes of the mother and daughter nuclei were assumed to be identical. This assumption is justified in most of regions of the nuclear chart except the transition regions. The calculated values for ^{49}Ar and ^{50}Ar are compared with the experimental data in Figs. 4(a),(b) and Figs. 4(c),(d), respectively. It can be seen in the figure that even though the experimental data suffer from large uncertainties the comparison with the calculations allows to draw some useful conclusions. For example, the experimental values for ^{49}Ar are consistent with a spherical shape of this nucleus with deformation parameter $\epsilon_2 \leqslant 0.1$. The ^{50}Ar nucleus is slightly deformed with the absolute value of the deformation between 0.1 and 0.2. It is impossible to determine the sign of the deformation, but the deformation is most likely oblate according to theoretical considerations [5,6,8,10,31,30].

The similar QRPA calculations for ^{48}Ar are presented in Figs. 4(e),(f). The recommended Q_β and S_n values for ^{48}Ar were taken from the literature [38] and were used in the calculations. Assuming that ^{46}Ar is a spherical nucleus [6] and ^{50}Ar is only weakly oblate, we can safely exclude the ground state deformation values for ^{48}Ar larger than $\epsilon_2 = \pm 0.1$, i.e., the nucleus is nearly spherical. This leads to a predicted half-life value in the the order of 550 ms and a neutron emission probability in the order of 30% [Figs. 4(e),(f)]. This value of the half-life is considerably different from the earlier QRPA prediction ($T_{1/2}=246$ ms [30,34]).

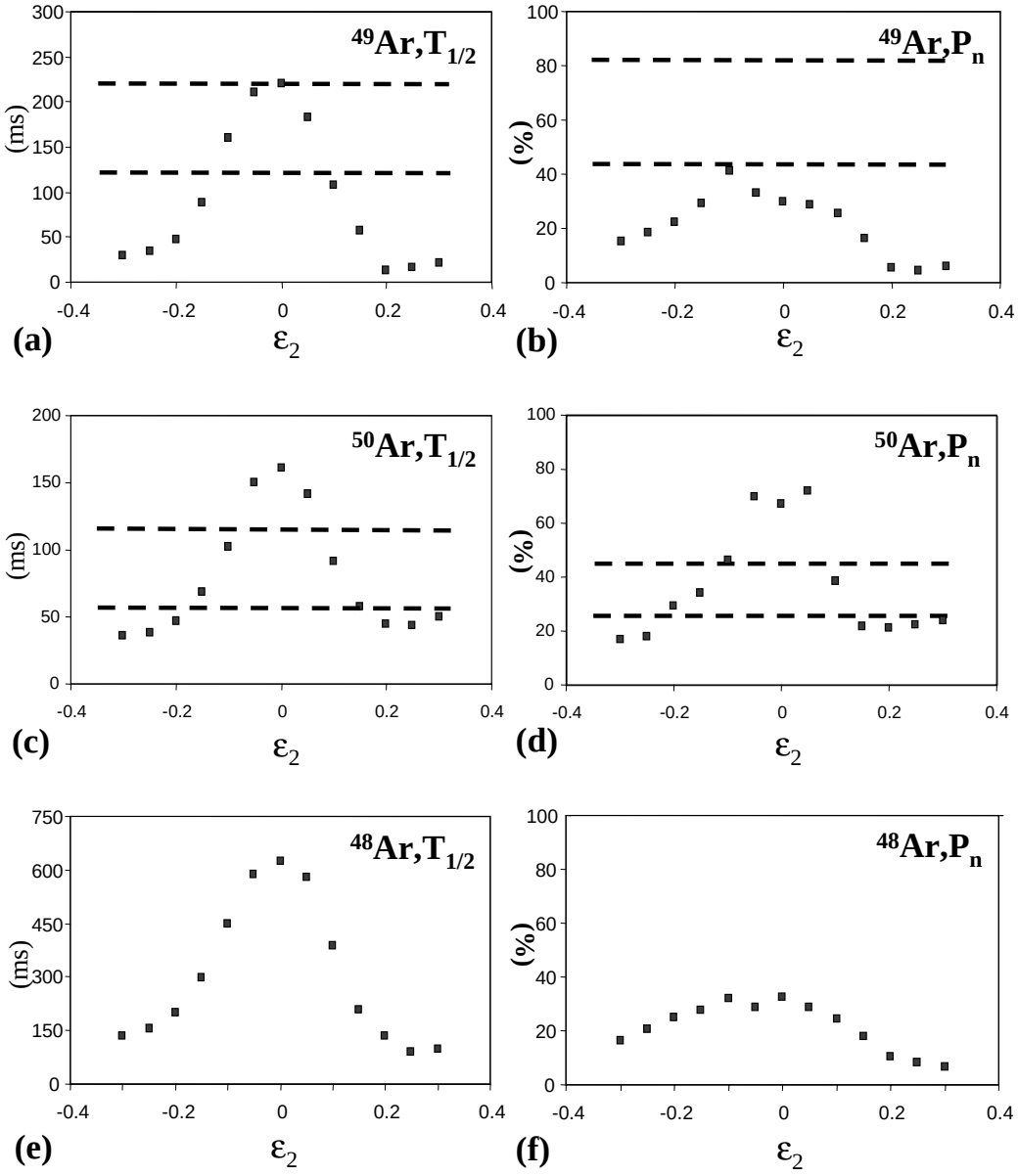

FIG. 4. Half-lives and P_n values calculated for different deformation parameters, ϵ_2, are compared with the experimental data for ^{49}Ar (a), (b) and ^{50}Ar (c), (d) nuclei. The similar calculations for the ^{48}Ar isotope are also presented (e), (f).

The new prediction of the ^{48}Ar half-life is in good agreement with the recently reported result from GANIL [39]. The obtained experimental values and the improved QRPA predictions can now be implemented in the astrophysical network calculations. Preliminary results of canonical *r*-process calculations indicate that the measured properties of the ^{49,50}Ar nuclei do not influence significantly the ^{48}Ca production and the ^{48}Ar isobar is the major progenitor.

IV. CONCLUSION

We have obtained new information on the gross β-decay properties of neutron-rich ^{49,50}Ar noble-gas isotopes using isobaric selectivity achieved by the combination of a plasma ion source with a cooled transfer line and subsequent mass separation. A doubly charged beam was used in the case of ^{49}Ar to suppress the corresponding multicharged background from noble gas symmetric fission products. At present, the measurement of decay properties with β and neutron decay time profiles is not possible for singly and doubly charged ^{48,47}Ar beams due to the multicharged SF background (see Fig. 1) and the singly charged ^{24}Ne contamination for the case of a doubly charged ^{48}Ar beam. On the other hand, using triply charged Ar beams will lead to further reduction of the yield by two orders of magnitude. As an alternative, one can consider the measurement of β-delayed γ rays from singly charged beams using comparison of the spectra obtained for $M=47,48$ with the corresponding γ spectra for $A=94,96$ and $A=141,144$ masses, identifying thus the γ rays originating from SF and ASF products.

The comparison of the ^{49,50}Ar data with the results of QRPA calculations indicates that the $N=28$ shell is not disturbed significantly for neutron-rich argon nuclei and these nuclei have only slight oblate deformation. As a consequence, the ground state shape of ^{48}Ar is expected to be nearly spherical. The obtained experimental results together with the improved model predictions are useful for a better understanding of the origin of ^{48}Ca/^{46}Ca isotopic anomaly discovered in inclusions from the Allende meteorite. The calculations are in progress.

ACKNOWLEDGMENTS

We would like to thank the crew of the PSB-ISOLDE facility for the operation of the separator and ion source. We are also grateful to Professor T. Glasmacher for his comments on the manuscript.

[1] O. Sorlin *et al.*, Nucl. Phys. **A583**, 763 (1995).
[2] O. Sorlin *et al.*, Phys. Rev. C **47**, 2941 (1993).
[3] H. Scheit *et al.*, Phys. Rev. Lett. **77**, 3967 (1996).
[4] T. Glasmacher *et al.*, Phys. Lett. B **395**, 163 (1997).
[5] T.R. Werner, J.A. Sheikh, W. Nazarewitcz, M.R. Strayer, A.S. Umar, and M. Misu, Phys. Lett. B **333**, 303 (1994).
[6] T.R. Werner, J.A. Sheikh, M. Misu, W. Nazarewitcz, J. Rikovska, K. Heeger, A.S. Umar, and M.R. Strayer, Nucl. Phys. **A597**, 327 (1996).
[7] K.-L. Kratz *et al.*, Phys. Bl. **51**, 183 (1995).
[8] J. Retamosa, E. Caurier, F. Nowacki, and A. Poves, Phys. Rev. C **55**, 1266 (1997).
[9] R.K. Gupta, S.K. Patra, and W. Greiner, Mod. Phys. Lett. A **12**, 1317 (1997).
[10] G.A. Lalazissis, D. Vretenar, P. Ring, M. Stoitsov, and L.M. Robledo, Phys. Rev. C **60**, 014310 (1999).
[11] T. Glasmacher, Annu. Rev. Nucl. Part. Sci. **48**, 1 (1998).
[12] P.D. Cottle and K.W. Kemper, Phys. Rev. C **58**, 3761 (1998).
[13] T. Lee, D.A. Papanastassiou, and G.J. Wasserburg, Astrophys. J. Lett. **220**, L21 (1978).
[14] F.R. Neiderer, Astrophys. J. Lett. **240**, L73 (1980).
[15] K.-L. Kratz *et al.*, Mem. Soc. Astron. Ital. **72**, 453 (2001).
[16] L.C. Carraz *et al.*, Phys. Lett. **109B**, 419 (1982).
[17] W. Ziegert, M. Wiescher, K.-L. Kratz, P. Möller, J. Krumlinde, F.-K. Thielemann, and W. Hillebrandt, Phys. Rev. Lett. **55**, 1935 (1985).
[18] W. Böhmer, Ph.D. thesis, University of Mainz, 1996.
[19] D. Guillemaud-Mueller *et al.*, Z. Phys. A **332**, 189 (1989).
[20] M.V. Ricciardi *et al.*, Nucl. Phys. **A701**, 156c (2002).
[21] A. Huck, G. Klotz, A. Knipper, C. Miehe, G. Walter, and C. Richard-Serre, Phys. Rev. C **21**, 712 (1980).
[22] P. Baumann, A. Huck, G. Klotz, A. Knipper, G. Marguier, H. Ravn, C. Richard-Serre, and G. Walter, Annual IRES report, Strasburg, 1989.
[23] U.C. Bergman *et al.*, Nucl. Phys. **A714**, 21 (2003).
[24] S. Sundell, H. Ravn, and ISOLDE Collaboration, Nucl. Instrum. Methods Phys. Res. B **70**, 160 (1992).
[25] R. Kirchner and E. Roeckl, Nucl. Instrum. Methods **133**, 187 (1976); Nucl. Instrum. Methods Phys. Res. B **70**, 160 (1992).
[26] U. Georg *et al.*, Nucl. Phys. **A701**, 137c (2002).
[27] U.C. Bergmann *et al.*, Nucl. Phys. **A658**, 129 (1999).
[28] U.C. Bergmann *et al.*, Eur. Phys. J. A **11**, 279 (2001).
[29] R.B. Firestone, *Table of Isotopes* (Wiley, New York, 1996).
[30] P. Möller, R. Nix, W.D. Myers, and W.J. Swiatecki, At. Data Nucl. Data Tables **59**, 181 (1995).
[31] Y. Aboussir, J.M. Pearson, A.K. Dutta, and F. Tondeur, Nucl. Phys. **A549**, 155 (1992).
[32] K.-L. Kratz, Nucl. Phys. **A417**, 447 (1984).
[33] J. Krumlinde and P. Möller, Nucl. Phys. **A417**, 419 (1984).
[34] P. Möller, J.R. Nix, and K.-L. Kratz, At. Data Nucl. Data Tables **66**, 131 (1997).
[35] P. Möller and J. Randrup, Nucl. Phys. **A514**, 1 (1990).
[36] K. Takahashi, M. Yamada, and T. Kondoh, At. Data Nucl. Data Tables **12**, 101 (1973).
[37] P. Möller, B. Pfeiffer, and K.-L. Kratz (unpublished), http://t16web.lanl.gov/Moller/publications/rspeed2002.html
[38] G. Audi and A. H Wapstra, Nucl. Phys. **A565**, 1 (1993).
[39] S. Grevy *et al.*, in Proceedings of ISPUN02, Halong, Vietnam, edited by S. Kubono and N. Dinh Dang [Nucl. Phys. A (to be published)].